

$E_0$  and  $F_0$ :

$$\begin{aligned} G_r(t) &= -i\theta(t)[E_0(\mathbf{k}, \mathbf{k}'; t) - F_0(\mathbf{k}, \mathbf{k}'; t)] \\ &= -i\theta(t) \int_{-\infty}^{\infty} e^{-ix't} [E_0(\mathbf{k}, \mathbf{k}'; x') - F_0(\mathbf{k}, \mathbf{k}'; x')] dx' \\ &= -i\theta(t) \int_{-\infty}^{\infty} e^{-ix't} (e^{\beta x'} - 1) F_0(\mathbf{k}, \mathbf{k}'; x') dx'. \quad (\text{A10}) \end{aligned}$$

The Fourier transform of  $G_r$  is

$$G_r(x) = \frac{1}{2\pi} \int_{-\infty}^{\infty} \frac{(e^{\beta x'} - 1) F_0(\mathbf{k}, \mathbf{k}'; x') dx'}{(x - x' + i\delta)}. \quad (\text{A11})$$

An expression for the Fourier transform of the advanced Green's function is obtained by changing the sign of  $\delta$  in this equation. Thus

$$\begin{aligned} (G_r - G_a) &= \frac{1}{2\pi} \int_{-\infty}^{\infty} (e^{\beta x'} - 1) F_0(\mathbf{k}, \mathbf{k}'; x') \\ &\quad \times \left[ \frac{1}{x - x' + i\delta} - \frac{1}{x - x' - i\delta} \right] dx' \\ &= -i(e^{\beta x} - 1) F_0(\mathbf{k}, \mathbf{k}'; x), \quad (\text{A12}) \end{aligned}$$

which is exactly Eq. (35) of the text.

## Optical Properties of 15R SiC: Luminescence of Nitrogen-Exciton Complexes, and Interband Absorption

LYLE PATRICK, D. R. HAMILTON, AND W. J. CHOYKE  
*Westinghouse Research Laboratories, Pittsburgh, Pennsylvania*  
 (Received 30 July 1963)

Optical experiments on 15R SiC are reported, and the results are compared with those given earlier for 6H SiC. The absorption edge is due to indirect, exciton-producing transitions, across an exciton energy gap of 2.986 eV at 6°K. Two distinct photoluminescence spectra are found, due to two kinds of nitrogen-exciton complexes. These spectra consist of series of lines, from which 18 phonon energies are obtained. Only four series of lines are observed in each spectrum, although there are five inequivalent nitrogen sites in 15R SiC. The four nitrogen donor ionization energies are found to be approximately 0.14, 0.16, 0.16, and 0.20 eV. These, and other binding energies, are somewhat smaller than in 6H SiC. As in the 6H SiC data, we find evidence of exciton hopping, of localized vibrations, of the presence of six conduction band minima, and of a second valence band, split off 4.8 meV by spin-orbit interaction.

### I. INTRODUCTION

UNTIL recently, the study of SiC polytype differences has been largely limited to x-ray investigations of the numerous stacking orders found in this material.<sup>1-3</sup> We are now reporting results of optical experiments on polytype 15R SiC, and we make many comparisons with results of similar experiments<sup>4,5</sup> on the most common SiC polytype, 6H. Since many SiC properties are nearly the same for all polytypes, it is interesting to speculate on the reasons for any marked differences.

Crystallographically, the SiC polytypes differ only in the stacking order (along the  $c$  axis) of close-packed atomic planes. The various polytypes can be represented by ordered sequences of the three letters,  $ABC$ , each

letter representing a plane of Si atoms, and another plane of C atoms. In this notation, rhombohedral 15R SiC (space group  $R3m$ ) is  $ABCACBCABACBCB$ ; hexagonal 6H SiC (space group  $P6_3mc$ ) is  $ABCACB$ . A short description of polytype structural differences is given in Sec. III.

The energy gaps of 6H and 15R SiC differ by only about 1%. That the difference is so little is probably accidental, for the energy gap of cubic SiC is considerably smaller,<sup>6</sup> and the energy gap of the 4H polytype is about 10% larger (see Fig. 1). All three polytypes shown in Fig. 1 have structure in their absorption edges which is characteristic of indirect optical transitions with the creation of excitons. In this respect they resemble Ge and Si.<sup>7</sup> The absorption edge of 15R SiC is shown in more detail in Sec. IX.

Considerable information on donors, phonons, and carriers in 6H SiC has been derived from recent studies

<sup>1</sup> A. R. Verma, *Crystal Growth and Dislocations* (Butterworths Scientific Publications Ltd., London, 1953), Chap. 7.

<sup>2</sup> R. S. Mitchell, *Z. Krist.* **109**, 1 (1957). This paper contains many references to x-ray results.

<sup>3</sup> P. Krishna and A. R. Verma, *Proc. Roy. Soc. (London)* **A272**, 490 (1963).

<sup>4</sup> W. J. Choyke and Lyle Patrick, *Phys. Rev.* **127**, 1868 (1962).

<sup>5</sup> D. R. Hamilton, W. J. Choyke, and Lyle Patrick, *Phys. Rev.* **131**, 127 (1963).

<sup>6</sup> Lyle Patrick, W. J. Choyke, and D. R. Hamilton, *Bull. Am. Phys. Soc.* **8**, 484 (1963). For cubic SiC,  $E_{G_0} = 2.39$  eV.

<sup>7</sup> G. G. Macfarlane, T. P. McLean, J. E. Quarrington, and V. Roberts, *Phys. Rev.* **108**, 1377 (1957); **111**, 1245 (1958); R. J. Elliott, *ibid.* **108**, 1384 (1957).

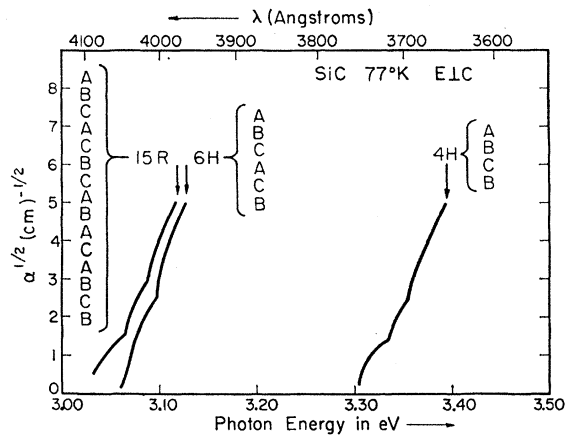


FIG. 1. Absorption edges of three SiC polytypes at 77°K (E1C), showing structure which is characteristic of indirect, exciton-creating transitions, with phonon emission.

of the photoluminescence of nitrogen-exciton complexes,<sup>4,5</sup> to be referred to here as CP and HCP. Much of this paper describes similar work on N-doped 15R SiC. We create excitons by uv illumination of the 15R samples at low temperatures. Excitons may be captured by neutral nitrogen to form four-particle complexes<sup>8</sup> (written ④), or by singly ionized nitrogen, to form three-particle complexes (③). The complexes decay by electron-hole annihilation, emitting photons, and, in most cases, one or more phonons. Two distinct spectra are observed. The four-particle spectrum lies from 0.007 to 0.127 eV below the exciton energy gap; the three-particle spectrum lies at somewhat lower energies. The two spectra overlap slightly, as indicated schematically in Fig. 2.

In both 6H and 15R polytypes, many of the unusual features of the photoluminescence are due to the large unit cells. The 15R unit cell contains 5 Si and 5 C atoms. Thus, there are five inequivalent sites<sup>9</sup> for N (which substitutes for C), and 30 branches in the phonon spectrum. This gives the possibility of observing, in the four-particle spectrum alone, five series of 31 lines each (including the no-phonon line). Actually, we have found only four series of lines, and 19 lines, at most, in a series. The number of lines resolved in the 15R spectra is about the same as in 6H. The origin of these lines is better understood if, instead of considering 30 phonon branches in the usual Brillouin zone, we consider six branches within a zone extended five times. Within the extended zone, the phonon spectrum has only *weak* singularities. This enables us to retain the usual notation, TA, LA, TO, and LO for the branches of the phonon spectrum.

<sup>8</sup> The ion is considered to be one particle, and the complex consists of the ion plus either three or two electronic particles. A fuller description of these complexes, and a comparison of our notation with Lampert's, is given in Table I of Ref. 5. See also M. A. Lampert, Phys. Rev. Letters **1**, 450 (1958); and J. R. Haynes, *ibid.* **4**, 361 (1960).

<sup>9</sup> Lyle Patrick, Phys. Rev. **127**, 1878 (1962).

There is a phonon spectrum associated with each type of complex. That obtained from the four-particle spectrum is characteristic of a loosely bound center, and that obtained from the three-particle spectrum is characteristic of a tightly bound center. These two phonon spectra are compared with each other, and with the similar spectra found in 6H SiC.

At higher temperatures, lines due to thermally excited states of the complexes are observed. The excited states of the four-particle complexes appear to be due to the presence of a second valence band (spin-orbit splitting). Those of the three-particle complexes are attributed to valley-orbit splitting; thus, the number of valley-orbit states found at 48°K leads us to conclude that the conduction band multiplicity is probably six.

The energies required to remove excitons from three or four-particle complexes are obtained directly from our spectra, and are found to be significantly smaller than the corresponding energies in 6H SiC. From these energies we can find a *lower limit* for the nitrogen donor ionization energies. Our experimental values for the 4 observed nitrogen donors (of an expected 5) are 0.118, 0.139, 0.139, and 0.179 eV. These energies are smaller than the nitrogen ionization energies in 6H SiC, and suggest that the effective electron mass is smaller in 15R SiC.

The presentation of the data is designed to facilitate comparisons with the parallel results for 6H SiC. Following the order in CP<sup>4</sup>, the four-particle spectrum is shown in Sec. V, and its relevance to the band structure is discussed in Sec. VI. Then, as in HCP<sup>5</sup>, the three-particle spectrum is shown in Sec. VII, and comparisons are made with the four-particle spectrum. The ionization energies of the nitrogen donors are discussed in Sec. VIII. Absorption measurements follow in Sec. IX, and then a summary, in Sec. X.

For convenience, and to help establish our notation, we shall repeat a number of equations used to define dissociation energies in HCP.

## II. NOTATION AND DISSOCIATION ENERGIES

In HCP we used the symbol ④ for a four-particle complex, ③ for a three-particle complex, and we continued the notation by using ② for a neutral donor, and ① for an ionized donor. Denoting electron, hole and exciton by  $e$ ,  $h$ , and  $x$ , we defined six dissociation energies by Eqs. (1) to (6).

$$\textcircled{4} \rightarrow \textcircled{3} + e - E_4, \quad (1)$$

$$\textcircled{3} \rightarrow \textcircled{2} + h - E_3, \quad (2)$$

$$\textcircled{2} \rightarrow \textcircled{1} + e - E_2, \quad (3)$$

$$x \rightarrow e + h - E_x, \quad (4)$$

$$\textcircled{4} \rightarrow \textcircled{2} + x - E_{4x}, \quad (5)$$

$$\textcircled{3} \rightarrow \textcircled{1} + x - E_{3x}. \quad (6)$$

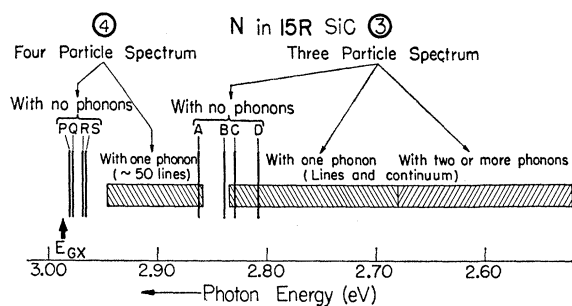


FIG. 2. A diagram, showing the energy ranges of the two distinct nitrogen-exciton luminescence spectra (four- and three-particle spectra), and indicating the positions of the four phonon-free lines in each spectrum.  $E_{Gx}$  is the forbidden gap energy for exciton creation.

These equations are not all independent. From them we derived the relations (7) and (8), from which, finally, (9) was obtained.

$$E_{4x} = E_4 + E_3 - E_x, \quad (7)$$

$$E_{3x} = E_3 + E_i - E_x, \quad (8)$$

$$E_i = E_{3x} - E_{4x} + E_4. \quad (9)$$

Since  $E_4$  is a positive quantity, we have a *lower limit* for the donor ionization energy  $E_i$ , namely

$$E_i > E_{3x} - E_{4x}. \quad (10)$$

The quantities  $E_{3x}$  and  $E_{4x}$  are accurately measured in the ③ spectrum and ④ spectrum respectively.

### III. POLYTYPES AND CRYSTAL GROWTH

Each SiC polytype has two identical interpenetrating sublattices of Si and C atoms. Each sublattice consists of an ordered sequence of close-packed planes of atoms, each plane having threefold symmetry about the stacking axis ( $c$  axis). Certain sequences permit a sixfold screw displacement operation,  $6_3$ , thus making possible the space group  $P6_3mc$ . One such sequence gives rise to the most common polytype,  $6H$ , with stacking order  $ABCACB$ . The  $15R$  polytype lacks the  $6_3$  operation, hence it has only a threefold axis (space group  $R3m$ ).

In both  $6H$  and  $15R$  polytypes the site symmetry, e.g., the symmetry of an N donor, which substitutes for C, is  $C_{3v}$ . All N donors in  $15R$  SiC are identical if one considers only nearest neighbors, of two kinds<sup>10</sup> when one takes second neighbors into consideration, and of 5 kinds<sup>11</sup> when one considers all neighbors.

With our usual crystal growing conditions,<sup>12</sup>  $6H$  is by far the most common SiC polytype, but some  $15R$  is nearly always present. The conditions favoring or

suppressing the growth of  $15R$  polytype are not yet understood. The crystals are usually (0001) platelets, and frequently the  $15R$  polytype is intergrown with  $6H$  in layers perpendicular to the  $c$  axis, occasionally with 2 or 3 layers in a crystal 1 mm thick.<sup>13</sup> Sometimes a pure  $15R$  portion may be isolated by grinding off one surface. Thicker crystals, with thick  $15R$  portions, have been grown in long furnace runs.

For absorption measurements the light may be directed perpendicular to the  $c$  axis, in which case a  $15R$  layer may be isolated by covering the  $6H$  portions with Aquadag. For photoluminescence it is necessary only to illuminate a  $15R$  surface.

In most of our crystals nitrogen is the most common *shallow* impurity, hence the largest contributor to the edge luminescence. The  $6H$  and  $15R$  nitrogen luminescence spectra include a number of characteristic narrow lines. Both  $6H$  and  $15R$  spectra may appear when a mixed crystal is illuminated, but no effect on linewidth or position has been observed, in either polytype, which could be attributed to a disordered or random structure. Thus, it appears that polytype changes during crystal growth are infrequent in our crystals. There is some x-ray evidence of random structures in the literature,<sup>14</sup> but perhaps these structures appear only under certain conditions of crystal growth.

### IV. 15R SAMPLES AND EXPERIMENTAL PROCEDURES

Although  $15R$  polytype is scarce, compared with  $6H$ , we found enough samples to make a survey of the luminescence spectra as a function of (1) nitrogen content, and (2) the degree of compensation by other impurities. As in  $6H$  SiC (HCP Sec. IV) the quenching of edge luminescence was considered to be evidence of exciton hopping in heavily doped samples; and the variations in the relative strengths of the ③ and ④ spectra correlated with the degree of compensation of the nitrogen. The survey enabled us to choose suitable samples for detailed examination at high spectral resolution (0.1 meV).

Our instruments and experimental procedures were the same as those reported in CP and HCP. Hence the samples were not immersed in helium, and the lowest temperature reached was again about 6°K.

### V. FOUR-PARTICLE SPECTRUM AT 6°K

#### A. Experimental Results

In this section we describe the photoluminescence spectrum of four-particle nitrogen-exciton complexes in  $15R$  SiC. From it we derive a phonon spectrum which

<sup>10</sup> The two kinds of sites are distinguished in the Jagodzinski notation,  $hkkhk$ , for  $15R$  polytype. This, and other common notations, are described in Ref. 1.

<sup>11</sup> The long, narrow, rhombohedral unit cell of  $15R$  has only 5 Si or C atoms, but extends 15 atomic layers along the  $c$  axis, hence, the designation  $15R$ .

<sup>12</sup> D. R. Hamilton, J. Electrochem. Soc. **105**, 735 (1958).

<sup>13</sup> The polytypes were determined in the first place by using an optical goniometer. In many samples the photoluminescence can now be used as a sensitive method of detecting polytypes.

<sup>14</sup> H. Jagodzinski and H. Arnold, in *Silicon Carbide*, edited by J. R. O'Connor and J. Smiltens (Pergamon Press, Inc., New York, 1960), p. 136. See also Ref. 3.

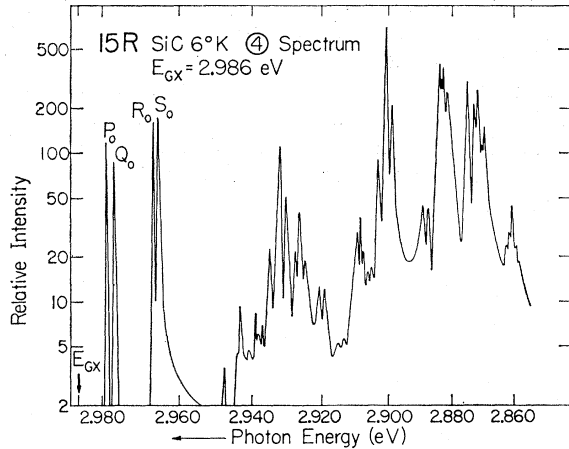


FIG. 3. Complete four-particle nitrogen-exciton luminescence spectrum at 6°K. The four phonon-free lines are marked  $P_0$ ,  $Q_0$ ,  $R_0$ , and  $S_0$ . The other lines, resulting from phonon emission, can be arranged in four series, each associated with one of the phonon-free lines.

will be interpreted by using an extended zone classification. The comparable results for 6H SiC are given in Sec. IV of CP.

Figure 3 shows the complete  $(4)$  spectrum at 6°K. The lines of the  $(4)$  spectrum are polarized, but information on polarization is not given in our drawings, and is not used in our interpretation.

Although there are five inequivalent sites for N in 15R SiC, only 4 series of lines have been found in the spectrum. The letters  $P$ ,  $Q$ ,  $R$ , and  $S$  are used to identify anything associated with a particular nitrogen site, such as the site itself, the  $(4)$  complex, and the series of lines emitted by the complex. In Fig. 3,  $P_0$ ,  $Q_0$ ,  $R_0$ , and  $S_0$  identify the 4 phonon-free lines, made possible by the localization of the exciton. These lines have a half-width of about 0.2 meV. With each is associated a series of lines through phonon emission, the phonons having the  $k$  values of the conduction band minima.

The phonon-free lines are displaced from  $E_{Gx}$  by the binding, or dissociation, energy defined as  $E_{4x}$  by Eq. (5) (the exciton energy gap,  $E_{Gx}$ , is 2.986 eV at 6°K, as derived from absorption measurements in Sec. IX). For  $E_{4x}$  we obtain, for  $P$ ,  $Q$ ,  $R$ , and  $S$  respectively, 7, 9, 19 and 20 meV. Because of these differences in  $E_{4x}$ , there are strong differences in the temperature dependence of the intensities of the four series of lines. Thus, by going to higher temperatures, one can easily identify the lines associated, through phonon emission, with each of  $P$ ,  $Q$ ,  $R$ , and  $S$ . The  $P$  and  $Q$  series are much stronger than the  $R$  and  $S$  series, and  $P$  is stronger than  $Q$ .

The lines emitted by the  $P$  complex, identified in the spectrum of Fig. 3 by the method described above, are shown alone in Fig. 4 to simplify the spectrum. The abscissa has been changed to measure displacements from the phonon-free line  $P_0$ . These displacements are measures of phonon energies; hence, we obtain from

TABLE I. A comparison of phonon energies in 15R and 6H SiC. Energies in meV.

TA		LA		TO		LO	
15R	6H	15R	6H	15R	6H	15R	6H
34.4	33.5	51.3	50.6	94.6	94.7	103.7	104.2
35.0	36.3	51.9	53.5	95.3	95.6	106.3	105.5
39.3	39.2	69.2	67.0	95.7	97.8	106.9	107.0
39.7	40.3	70.2	69.0	97.1			
43.2	44.0	78.2	77.0				
46.3	46.3						

Fig. 4 a spectrum of 18 phonon energies out of a theoretically possible 30. A small portion of the  $P$  series is shown in Fig. 5 to indicate the degree of resolution of some of these lines. One reason we do not find more phonon energies is probably that we cannot resolve all double or multiple peaks.

The phonon spectrum derived from another series, ( $Q$ ,  $R$ , or  $S$ ), is found to be the same, within experimental error, so we consider only the  $P$  series from now on. For 6H SiC (CP Sec. VI) the  $(4)$  phonon energies were equal, within experimental error, to lattice phonon energies found in the intrinsic spectrum (the intrinsic spectrum is that which is due to the decay of free excitons). In 15R SiC we do not see the intrinsic spectrum, but we assume that the  $(4)$  phonon energies are again those of lattice phonons. A classification of the phonon energies is made in Sec. VI by plotting the energies against wave vector in an extended zone. The wave vectors are not determined experimentally, but are chosen in a manner to be explained later.

The 18 phonon energies are given in Table I, together with those of 6H SiC for comparison. The near co-

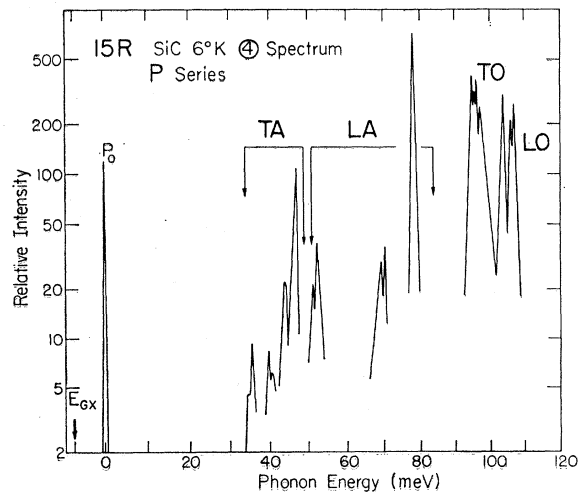


FIG. 4. One of the four series of luminescence lines shown in Fig. 3, the  $P$  series. By selecting one series we avoid the complication due to inequivalent nitrogen sites. The zero of energy has been placed at  $P_0$ , so that the energies of emitted phonons may be read directly from the abscissa. The grouping of phonons (into TA, LA, TO, and LO) is made possible by use of an extended zone.

incidence of many 15R and 6H phonon energies is rather surprising, in view of the fact that the symmetry, and hence the extended zones, are different. This near coincidence explains our failure to distinguish between 6H and 15R SiC in our infrared spectra of the two-phonon combination bands.<sup>15</sup>

### B. The Fifth Nitrogen Donor

There is evidence that the 3 nitrogen sites are equally populated in 6H SiC.<sup>16</sup> One would expect the 5 nitrogen sites of 15R SiC also to be equally populated, yet we observe only four series of lines in the ④ spectrum. The following is a possible explanation of the missing fifth series.

Relative intensities in the four observed series of lines are found to depend on the energies  $E_{4z}$  in two ways. (1) The phonon-free lines,  $P_0$ ,  $Q_0$ ,  $R_0$ , and  $S_0$ , owe their existence to the localization of the exciton.  $R$  and  $S$  sites have binding energies,  $E_{4z}$ , roughly twice those of  $P$  and  $Q$ ; hence, the percentage of phonon-free transitions in the  $R$  and  $S$  series is considerably greater. (2) The relative capture cross sections of the four nitrogens, obtained by considering the intensities summed over all lines of a series, diminish with increasing  $E_{4z}$ . These two factors were also noted in 6H SiC, and were discussed more fully in Sec. IV D of CP. It follows that, if  $E_{4z}$  were large enough, one might observe not a series of lines, but only a single weak phonon-free line.

In our samples we find two lines which do not belong to the  $P$ ,  $Q$ ,  $R$ , or  $S$  series. One of these may be the phonon-free line of the fifth nitrogen. Another possibility, which we consider very unlikely, is that the fifth  $E_{4z}$  is too small to bind an exciton at 6°K.

## VI. EXTENDED ZONE AND BAND STRUCTURE

### A. The Extended Zone

The rhombohedral unit cell of 15R SiC is a long, narrow cell, stretching 15 layers along the  $c$  axis. It holds 5 Si and 5 C atoms. Thus, the Brillouin zone is highly compressed in the  $c$  direction, and there are 30 phonon branches. It is more convenient to use a zone extended five times along the  $c$  axis. This reduces the number of phonon branches to the usual six, denoted by TA (2), LA, TO (2), and LO. The effect of the complex stacking order is then to introduce, within the extended zone, planes of energy discontinuity perpendicular to the  $c$  axis, at multiples of  $\pi/c$ . However, the energy gaps at these discontinuities are very small compared with the gaps at the boundary of the extended zone at  $5\pi/c$ .

Within the extended zone there are electron or phonon states connected by the reciprocal lattice vec-

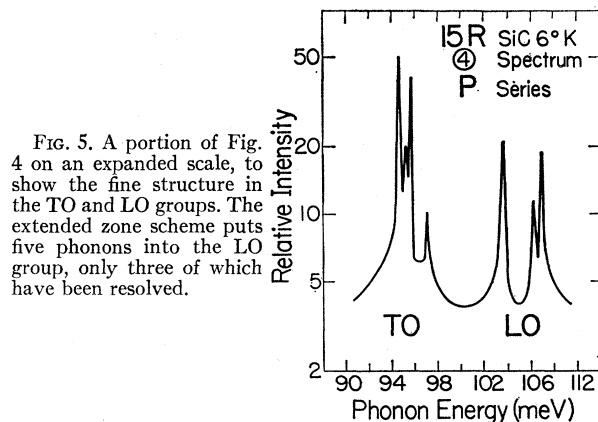


FIG. 5. A portion of Fig. 4 on an expanded scale, to show the fine structure in the TO and LO groups. The extended zone scheme puts five phonons into the LO group, only three of which have been resolved.

tor  $2\pi/c$ ; one may also think of such states as being mixed by a "superlattice" potential due to the complex stacking order.

### B. Conduction Band Minima

In 15R SiC, as in 6H SiC, the most intense TA and LA phonons are those of highest energy, suggesting that the conduction band minima are on the extended zone boundary, with  $k_c = 5\pi/c$ . To the other phonons we assign wave vectors differing by multiples of the reciprocal lattice vector  $2\pi/c$ , i.e., vectors with components  $k_c = 3\pi/c$  and  $k_c = \pi/c$ . In this, and in the assignments of  $k_c$  to TO and LO phonons, we are guided by plausibility arguments, and by the similarities with the 6H phonon spectrum. The result is the plot shown in the left portion of Fig. 6.

If we are correct in our wave vector assignments, the general appearance of the phonon plot depends strongly on how far the conduction band minima lie from the  $c$  axis. If they were far from the  $c$  axis, the three  $\mathbf{k}$  vectors would be comparable in magnitude, as illustrated in Fig. 7; hence, the energies in any one phonon branch would also be comparable, and a phonon spectrum with  $k_c$  as abscissa would appear strongly distorted. Comparing Fig. 6 with Fig. 5 of CP, which shows the ④ phonon spectrum of 6H SiC, we conclude that the conduction band minima are probably somewhat farther from the  $c$  axis in 15R than in 6H.

For 6H SiC, the ④ spectrum suggested a sixfold conduction band degeneracy, and the sixfold degeneracy seems to be confirmed by the appearance of 6 lines in the valley-orbit splitting of the ③ spectrum (HCP, Sec. IX). There should also be six conduction band minima in 15R SiC, if the minima lie on mirror planes, at the zone boundary, for there is threefold symmetry about the  $c$  axis, and a doubling of minima due to the condition  $E(\mathbf{k}) = E(-\mathbf{k})$ . In 15R we have seen only five lines due to valley-orbit splitting of the ③ spectrum (Sec. VII B), but we are limited, in this experiment, by the strong temperature dependence of the luminescence intensity.

<sup>15</sup> Lyle Patrick and W. J. Choyke, Phys. Rev. **123**, 813 (1961).

<sup>16</sup> H. H. Woodbury and G. W. Ludwig, Phys. Rev. **124**, 1083 (1961).

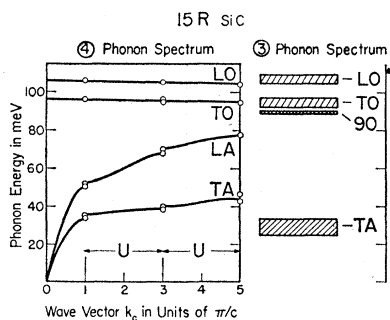


FIG. 6. A comparison of phonon energies derived from the four-particle and three-particle spectra. The narrow four-particle lines have been assigned  $\mathbf{k}$  values, as explained in the text. The broad three-particle lines probably represent large regions in  $\mathbf{k}$  space. The heights of the boxes indicate the approximate half-widths of these lines. The 90-meV phonon appears to fall between the acoustic and optical branches, and may be a localized vibration.

### C. Valence Band Structure

The changes observed in the (4) spectrum, as one goes to higher temperatures, are very similar to those reported in Sec. V of CP for 6H SiC. (1) The  $P$  and  $Q$  series disappear at about 20°K because of the small binding energies,  $E_{4z}$ . (2) Duplicate  $R$  and  $S$  lines appear, due to a thermally excited state of the (4) complex. These new lines are displaced 4.8 meV, and have the same polarization as the lines from which they are displaced, exactly as in 6H SiC. We therefore attribute them to the presence of a second valence band, split off by spin-orbit interaction. We saw no sign of a third valence band. It is reasonable to suppose that the valence band structure of 15R is very similar to that of 6H, which is discussed at length in CP. Thus, for example, holes are thought to be largely confined to the carbon sublattice.

## VII. THREE-PARTICLE SPECTRUM

An exciton is bound to a nitrogen ion with an energy,  $E_{3z}$ , which is an order of magnitude greater than the binding energy  $E_{4z}$  to a neutral nitrogen. Some of the consequences are (a) the (3) spectrum is displaced to lower energies, as shown in Fig. 2; (b) phonon energies represent a larger region in  $\mathbf{k}$  space, hence photon lines are broadened; (c) stronger interaction with the lattice leads to multiphonon emission; and (d) the (3) spectrum can be observed at temperatures high enough to quench the (4) spectrum. These effects were all previously observed in 6H SiC (see HCP).

### A. Experimental Results at 6°K

Figure 8 shows a large portion of the (3) spectrum at 6°K. The spectrum consists of four series of lines, called  $A$ ,  $B$ ,  $C$ , and  $D$ . The expected fifth series cannot be seen. Each series has a narrow, phonon-free line, and a number of broader lines displaced to lower ener-

gies by phonon emission. For example, peaks A30 to A90 involve emission of phonons of 30 and 90 meV by the  $A$  complex. As one goes to lower energies, toward the right of Fig. 8, the resolution of the peaks becomes increasingly poorer. This is due to increasing overlap of the four series of lines, and the appearance of broad two-phonon bands (and, eventually, of multiphonon bands).

Good resolution is obtained only for the  $A$  and  $B$  series, for which the phonon energies are the same, except for some fine structure. The phonon spectrum is also the same as the (3) phonon spectrum of 6H SiC, except for fine structure, and the non-observance of a 60-meV phonon which was considered rather doubtful in the 6H spectrum (see Fig. 5 of HCP).

The (3) phonon spectrum is shown at the right of Fig. 6 for comparison with the (4) phonon spectrum. The heights of the bars indicate the approximate half-widths of the lines. As in 6H SiC, the narrow 90-meV phonon appears to lie in the gap between acoustic and optical branches, and may represent a localized vibrational mode.

The fine structure cannot be shown in Fig. 8 because of the scale. The lines  $A$ ,  $B$ , and  $D$  are doublets, with line separation 1 to 2 meV. The relative strengths of the two lines in a doublet is a function of temperature, as described in HCP for the similar doublets found in the (3) spectrum of 6H SiC. Additional temperature dependent peaks are described in the next section.

The A94 and B94 peaks also show fine structure, but it is not as well resolved as in the comparable peaks of 6H SiC. This fine structure, is, no doubt, a reflection of the fact that there are ten TO branches in the conventional Brillouin zone, but we have not been able to make a correlation between the components of the

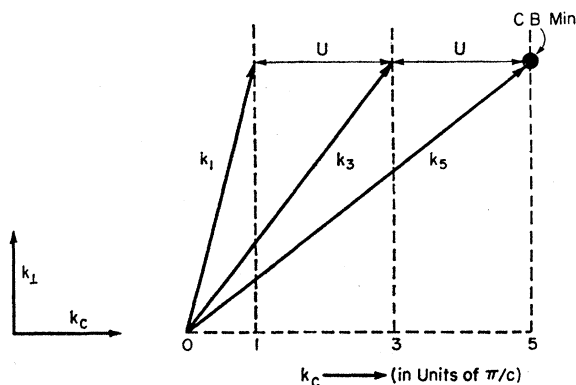


FIG. 7. A plane in  $\mathbf{k}$ -space, illustrating relationships between wave vectors of momentum-conserving phonons. If a conduction band minimum is located as shown in the figure, and if the valence band maximum is at  $\mathbf{k}=0$ , then the wave vector  $\mathbf{k}_5$  connects the two directly. The vectors  $\mathbf{k}_1$  and  $\mathbf{k}_3$  are related to  $\mathbf{k}_5$  by reciprocal lattice vectors ( $U$ ). It is evident that the wave vector  $\mathbf{k}_1$  in particular, and the corresponding phonon energy, are strong functions of the distance of the conduction band minima from the  $c$  axis, assuming that they lie on the plane  $k_c = 5\pi/c$ .

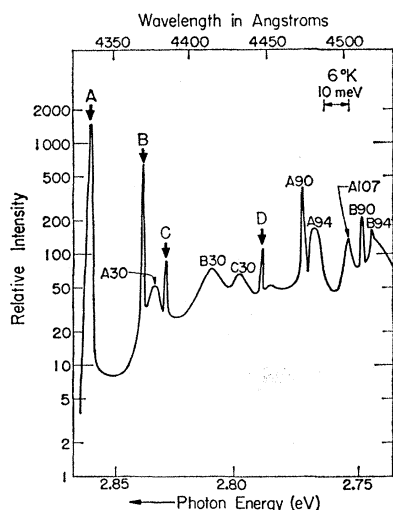


FIG. 8. A large portion of the three-particle spectrum at 6°K. A, B, C, and D are phonon-free lines. Other lines are identified by series letter and phonon energy in meV. The fine structure is not resolved in this figure.

94-meV peak and the well-resolved TO peaks of the ④ spectrum.

The higher energy series, A and B, are an order of magnitude more intense than C and D. If the missing fifth series falls at lower energy and is weaker still, it could very well escape detection. The fifth no-phonon line may be hidden by the strong A90 or A94 peaks.

### B. Experimental Results at 48°K

Additional temperature-dependent lines in the ③ spectrum, like those in the ③ spectrum of 6H SiC, are attributed to thermally excited states of the ③ complex. The excited states are thought to be due to valley-orbit splitting,<sup>17</sup> for the reasons given in Sec. VIII of HCP for 6H. The A nitrogen has the smallest ionization energy and so should be most favorable for the observation of additional valley-orbit lines (again, as in 6H). We do, in fact, find five no-phonon lines for A at 48°K, as shown in Fig. 9, but no temperature-dependent lines for the other nitrogens, except the upper lines of the B and D doublets.

In 6H SiC the A complex emits six lines at 77°K. In 15R SiC we are unable to make any measurements at 77°K, because of thermal quenching of the spectrum. Even at 48°K the intensity is low, so conditions are unfavorable both for thermally exciting and for observing the upper states. However, we can say that there are at least five energy levels, hence, in view of the symmetry requirements, at least six conduction band minima.

It seems probable that there are exactly six conduction band minima, perhaps giving rise to two  $\Lambda_1$  non-degenerate valley-orbit states, and two  $\Lambda_3$  doubly degenerate states. The observation of doublets for A, B, and D, with splittings comparable to those of the A and C doublets of 6H SiC, leads us to believe that

these result from Jahn-Teller splitting of  $\Lambda_3$  states.<sup>18</sup> Hence, we tentatively assign the observed lines to  $\Lambda_1$  and  $\Lambda_3$  states as indicated in Fig. 9.

In both 15R and 6H SiC,  $E_3 < E_{3x}$ , hence we expect that both ③ spectra are quenched when ③ complexes dissociate into holes and neutral nitrogens. Thus, the fact that the 15R three-particle spectrum disappears at a lower temperature than that of 6H SiC probably indicates that  $E_3$  is smaller in 15R SiC. We shall compare a number of dissociation energies in these two polytypes in the next section.

### VIII. IONIZATION AND DISSOCIATION ENERGIES

The donor ionization energies are given by Eq. (9), and a lower limit is  $E_{3x} - E_{4x}$ , which is just the energy difference between corresponding phonon-free lines in the ③ and ④ spectra. For the purpose of estimating  $E_i$ , we assume, as we did for 6H SiC, and as suggested by Haynes' results for Si,<sup>8</sup> that the lines should be paired in the order of their energies, i.e., A with P, B with Q, C with R, and D with S. This assumes, for example, that one of the five inequivalent nitrogens emits the A series as a ③ complex, and the P series as a ④ complex. The missing fifth series in each spectrum probably corresponds to the largest values of  $E_{3x}$  and  $E_{4x}$ , hence, to values that would be paired under our procedure. Since the four measured values of  $E_{4x}$  fall within 13 meV, our pairing order cannot, in any case, introduce any larger error into the "Minimum  $E_i$ " shown in Table II.

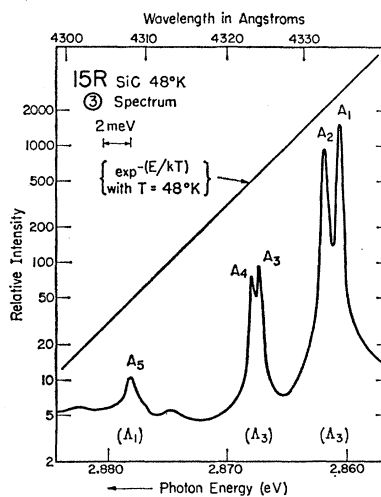


FIG. 9. A small part of the three-particle spectrum at 48°K. The lines  $A_1$  and  $A_2$  correspond to the single line A in Fig. 8, but  $A_2$  is relatively stronger at 48°K. Lines  $A_3$ ,  $A_4$  and  $A_5$  are not observed at 6°K. Their intensities are given roughly by the Boltzmann factor, shown by the sloping straight line. These peaks are attributed to thermally excited states of the A complex which are thought to be due to valley-orbit splitting.

<sup>17</sup> W. Kohn, in *Solid State Physics*, edited by F. Seitz and D. Turnbull (Academic Press Inc., New York, 1957), Vol. 5, p. 257.

<sup>18</sup> See HCP Sec. IX for a discussion of the comparable splittings in 6H SiC.

TABLE II. A comparison of 15R and 6H nitrogen donor ionization energies, and the energies  $E_{4z}$  and  $E_{3z}$  defined by Eqs. (5) and (6). Energies in eV.

	$E_{4z}$	$E_{3z}$	Minimum $E_i$ $E_{3z} - E_{4z}$	Probable $E_i$
15R	P 0.007	A 0.125	0.118	0.14
	Q 0.009	B 0.148	0.139	0.16
	R 0.019	C 0.158	0.139	0.16
	S 0.020	D 0.199	0.179	0.20
6H	P 0.016	A 0.162	0.146	0.17
	R 0.031	B 0.203	0.172	0.20
	S 0.033	C 0.237	0.204	0.23

To obtain a "probable" value for  $E_i$ , we simply add 20 meV to the "minimum" value, this being an estimate of the energy  $E_4$  of Eq. (9). The rather lengthy argument for this estimate will not be given here, as it parallels that of HCP (Sec. VI) for 6H SiC.

A comparison of  $E_{4z}$ ,  $E_{3z}$  and  $E_i$  for 6H and 15R SiC is given in Table II. One of the most significant differences between the two polytypes is that these dissociation energies are smaller in 15R. The hydrogenic approximation cannot be considered good in SiC, but, nevertheless, it suggests that the lower values of  $E_i$  in 15R SiC may be a consequence of a smaller electron mass. If so,  $E_x$  should also be smaller. But Eq. (7) shows that  $E_3 + E_4 = E_x + E_{4z}$ , hence, the sum on the left would also be smaller in 15R SiC. We indicated in Sec. VII B that a smaller value of  $E_3$  is the probable reason for the stronger thermal quenching of the  $\textcircled{3}$  spectrum in 15R SiC. Thus, a smaller effective mass for the electron may lead to lower values of five, and

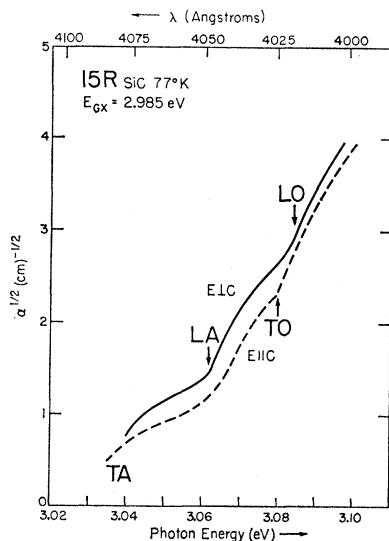


FIG. 10. The two absorption edges of 15R SiC, at 77°K, using polarized light. The structure is characteristic of indirect, exciton-producing transitions. At 77°K only the phonon *emission* part is observed. At least 18 phonons are involved, in this energy range, but the principal structure is due to a smaller number, as explained in the text.

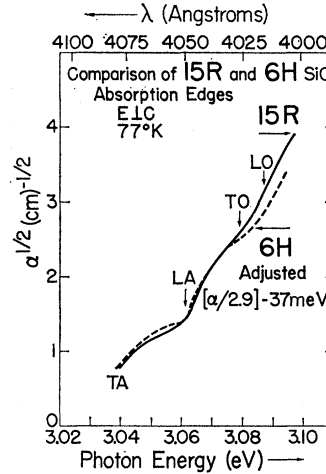


FIG. 11. Comparison of the  $E_{\perp C}$  absorption edges of 15R SiC (solid line) and 6H SiC (broken line) at 77°K. The abscissa and ordinate refer only to the 15R curve. The 6H absorption coefficients have been divided by 2.9, and the 6H curve has been translated along the energy axis by 37 meV.

perhaps all six of the dissociation energies defined by Eqs. (1) to (6).

## IX. ABSORPTION SPECTRUM

The absorption edge of 15R SiC is similar in shape to that of 6H, but the absorption strength is less by a factor 3. The similarity in shape can be explained by using the results of the luminescence experiments, but we can only speculate on the intensity difference.

Figure 10 shows the two absorption edges of 15R SiC, using polarized light, at 77°K. At this temperature only indirect transitions with phonon *emission* are significant. We have plotted the square root of the absorption coefficient ( $\alpha^{1/2}$ ) against photon energy, as is usually done for indirect transitions. Such a plot becomes linear at higher photon energies.<sup>19</sup> However, the portion of the edge shown in Fig. 10 is that in which excitons are formed, rather than free electrons and holes.<sup>20</sup> With increasing photon energy, the 18 or more phonons become effective in the order of their energies, thus, causing a great deal of structure in the absorption edge, much of it not resolved. The acoustic phonons at the extended zone edge are the most prominent, as they are in the luminescence, so that the principal structure is due to these, and to the optical phonons. The energies at which these phonons become effective are identified in Fig. 10 by arrows and appropriate labels TA, LA, TO, and LO.

The phonon energies can be obtained from the luminescence measurements with much greater accuracy than from the absorption measurements. We merely note that there are no inconsistencies. We use the absorption measurements to find the exciton energy gap. We find  $E_{Gx} = 2.985$  eV at 77°K (2.986 eV at 6°K).

<sup>19</sup> A more detailed account of absorption is given for 6H SiC in CP, most of which applies, with only small changes, to 15R SiC also.

<sup>20</sup> T. P. McLean, in *Progress in Semiconductors* (Heywood and Company Ltd. London, 1960), Vol. 5, p. 55.



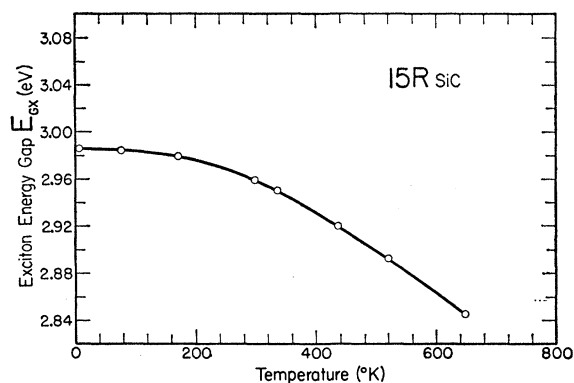


FIG. 12. The exciton energy gap  $E_{Gx}$  as a function of temperature. The points were obtained from absorption measurements. A linear dependence on temperature is probably observed only at a still higher temperature.

The usual energy gap  $E_G$  is larger than  $E_{Gx}$  by the still unknown exciton binding energy  $E_x$ .

A comparison of 15R and 6H absorption edges is shown in Fig. 11. The abscissa and ordinate refer to the solid line 15R curve (for  $E \perp c$ ). The 6H curve has been displaced by 37 meV ( $E_{Gx}$  for 6H SiC is 3.023 eV), and the 6H absorption coefficient,  $\alpha$ , has been divided by 2.9 to bring the curves into near agreement. The energies of the phonons most effective in determining the structure of the edges are the same, as one would expect from the luminescence results (Table I). There is some difference in the relative effectiveness of the acoustic and optical phonon branches, but one may say that the 6H absorption intensity is roughly three times that of 15R.

The many factors determining the absorption intensity are discussed in Ref. 20. Among them are matrix elements for photon and for phonon transitions, conduction band multiplicities, and various densities of states. The photon transitions occur either at  $\mathbf{k}=0$  or  $\mathbf{k}=\mathbf{k}_{cb}$ . Thus, four densities of electron or hole states are involved,<sup>21</sup> but our luminescence measurements enable us to make some comparisons of only two of these. A conduction band effective mass smaller in 15R by 10 or 20%, as suggested by the nitrogen

<sup>21</sup> More than four densities of states are involved if one considers transitions to all intermediate states.

ionization energies, cannot account for the factor 3 (absorption is proportional to the density of states, which is proportional to  $m^{3/2}$ ). The factor 3 must, therefore, be attributed to one or more of the many unknowns.

Figure 12 shows the change of  $E_{Gx}$  with temperature, obtained from absorption measurements by observing, at low temperatures, the break in the curve which indicates the beginning of the phonon emission part; and at high temperatures the break which indicates the beginning of the phonon absorption part. All structure in the absorption edge becomes less distinct with increasing temperature, hence, the high temperature portion of Fig. 12 is somewhat uncertain.

## X. SUMMARY

The photoluminescence spectra due to the two kinds of nitrogen-exciton complexes in 15R SiC are very similar to those of 6H SiC, and yield very similar phonon spectra. However, ionization energies and other binding energies are generally smaller in 15R, perhaps due to a smaller electron mass. Only four of the five inequivalent nitrogens in 15R SiC have been detected.

The absorption edges of 15R SiC are due to indirect transitions which produce excitons. The edges are similar in shape to those of 6H SiC, which is not surprising, in view of the similarity of the phonon spectra. However, a factor of 3 difference in intensity of absorption has not been explained. The 15R exciton energy gap is 2.986 eV at 6°K, 0.037 eV smaller than that of 6H SiC.

From the luminescence of thermally excited states of the ④ complexes, we conclude that 15R SiC has a second valence band, split off by 4.8 meV, due to spin-orbit interaction, and that holes are largely confined to the carbon sublattice.

Thermally excited states of the ③ complex are thought to be due to valley-orbit splitting, and suggest a sixfold conduction band degeneracy. The band structure evidence and the conclusions are very similar to those given earlier for 6H SiC.

## ACKNOWLEDGMENT

We wish to thank M. M. Sopira, Jr., for technical assistance.